Chemical Engineering Journal 163 (2010) 180–187

Contents lists available at ScienceDirect

Chemical Engineering Journal

journal homepage: www.elsevier.com/locate/cej

Review

Enhanced micromixing of electroosmotic flows using aperiodic time-varying zeta potentials

Ching-Chang Cho, Ching-Jenq Ho, Cha'o-Kuang Chen *

Department of Mechanical Engineering, National Cheng Kung University, No. 1, University Road, Tainan 70101, Taiwan, ROC

ARTICLE INFO

Article history:
Received 22 February 2010
Received in revised form 28 July 2010
Accepted 2 August 2010

Keywords:
Micromixer
Active mixing
Electroosmotic flow
Microchannel
Numerical analysis

ABSTRACT

This paper proposes a technique for enhancing the mixing of electroosmotic flows in a microchannel by means of aperiodic spatio-temporal variations in the zeta potential. The effects of the magnitude of the time-varying zeta potential, the length of the heterogeneous surface zeta potential patterns, and the aperiodic switching frequency of the zeta potential on the fluid flow characteristics and mixing performance are analyzed by performing a series of numerical simulations in which the aperiodic oscillating source used to modulate the switching frequency of the zeta potential over time is derived using the Sprott system. The results show that the aperiodic spatio-temporal variations in the zeta potential generate irregularly alternating flow recirculations over time, which in turn produce a stirring of the species. In addition, it is shown that an effective enhancement in the mixing performance can be obtained through the application of a suitable switching frequency. Moreover, the mixing performance can be further improved by increasing the strength of the heterogeneous surface zeta potential or the length of the heterogeneous surface zeta potential patterns, respectively. Overall, it is shown that an average mixing efficiency of over 90% can be obtained when the length of the heterogeneous surface zeta potential patterns is equal to twice the channel width, the magnitude of the heterogeneous surface zeta potential is twice that of the homogeneous surface zeta potential, and the value of the oscillating frequency used to modulate the variation of the zeta potential is assigned within an appropriate range.

1. Introduction

The rapid advancement of micro-electro-mechanical systems (MEMS) techniques in recent decades now makes possible the integration of multiple microfluidic devices on a single chip to accomplish micro-total analysis systems (μ-TAS) for chemical and biological analysis purposes. Generally speaking, the performance of such systems is reliant upon an efficient mixing of the species. However, due to the small characteristic scale of microfluidic devices, the species flow is constrained to the low Reynolds number regime. As a result, the fluid flow is laminar and species mixing occurs primarily as the result of diffusion. Therefore, in the absence of turbulence, a thorough mixing of the species requires both a long mixing length and a long mixing time. However, neither requirement is compatible with the general goals of microfluidic systems, namely miniaturization and a high throughput. Consequently, a requirement exists for more efficient micromixing schemes capable of achieving a thorough species mixing within a short mixing length and a short mixing time.

In general, the proposals presented in the literature for efficient micromixing strategies can be classified as either passive or active, depending on the manner in which the species are mixed. In passive mixing schemes, the species are mixed through the flow disturbances induced by the specific geometric features of the microchannel, and no additional force is required to perturb the species other than that required to actually drive them through the device. Typical passive micromixers include staggered herringbone mixers [1–3], three-dimensional serpentine mixers [4–6], split-and-recombine mixers [7,8], and zigzag/waveform mixers [9–11]. In contrast to passive mixing schemes, active mixing strategies utilize an external perturbing force or mechanical components to perturb the species, thereby achieving a mixing effect. Typically, the species perturbation is achieved by utilizing a periodic oscillating velocity or pressure to generate transverse flows within the microchannel. Many studies have shown that by specifying the operating conditions in such a way as to achieve chaotic flow, the active mixing strategies yield an efficient species mixing as a result of the repeated stretching and folding of the sample streams at the interface between them [12–14].

In recent years, electrokinetic techniques have emerged as the method of choice for species mixing in microfluidic systems. Compared to traditional pressure-driven mixing schemes, electrokinetic methods have a number of key advantages, including

* Corresponding author. Tel.: +886 6 2757575x62140; fax: +886 6 2342081.
E-mail address: ckchen@mail.ncku.edu.tw (C.-K. Chen).

1385-8947/$ – see front matter © 2010 Elsevier B.V. All rights reserved.
doi:10.1016/j.cej.2010.08.003

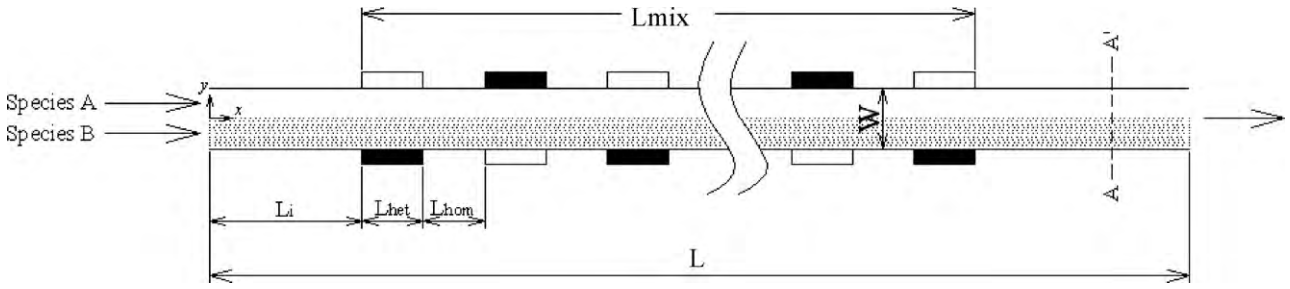

Fig. 1. Schematic illustration showing micromixer configuration. Note that the filled and unfilled blocks represent heterogeneous surface zeta potential surfaces.

the ability to manipulate tiny volumes of sample with an extremely high degree of precision, a lack of moving parts, a straightforward integration with other microfluidic devices, and so on. In [15,16], a periodically varying electric field was applied to the side channels of a T-/cross-shaped micromixer such that the two species were injected alternately into the main microchannel. It was shown that the mixing efficiency could be enhanced by increasing the interfacial contact area between the two species by applying a suitable switching frequency. Some researchers have demonstrated that the mixing performance can be further improved by utilizing time-varying externally applied electric fields to perturb the species within the microchannel. For example, in [17,18], sinusoidally alternating external electric fields were applied to species with different conductivities in order to produce an instability phenomenon within the species, while in [19], periodic electric fields with a 90-degree phase shift were applied to the electrodes at the ends of closed lateral channels in order to excite vortices. In [20], a complex flow behavior was induced by applying random perturbations to the time-periodic electric field used to drive the species. Finally, in [21,22], harmonic and chaotic electric fields were applied to the electrodes of a mixing chamber to produce periodic and aperiodic perturbation effects within the chamber.

In addition to the active techniques described above, some researchers have shown that an enhanced mixing performance can be obtained by applying non-uniform zeta potentials along the length of the mixing channel in order to induce local flow recirculations [23,24]. In contrast to passive mixing methods in which non-uniform time-independent zeta potentials are applied along the channel wall [25–27], the application of non-uniform time-varying zeta potentials to local regions of the channel surface yields a more efficient mixing performance since the resulting flow recirculation structures vary over time and therefore generate a more

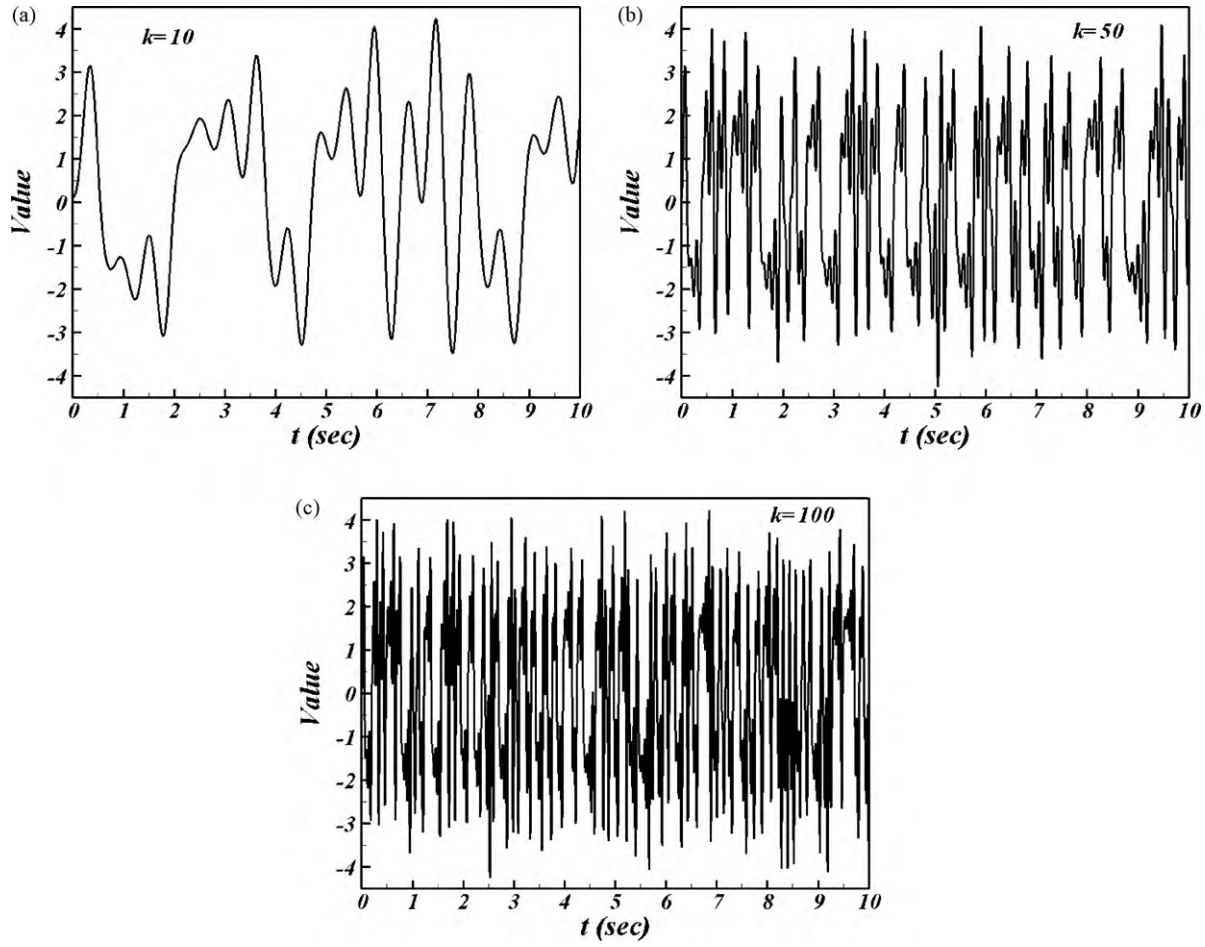

Fig. 2. Oscillatory orbits in Sprott system with scaling factors of: (a) $k = 10$, (b) $k = 50$, and (c) $k = 100$.

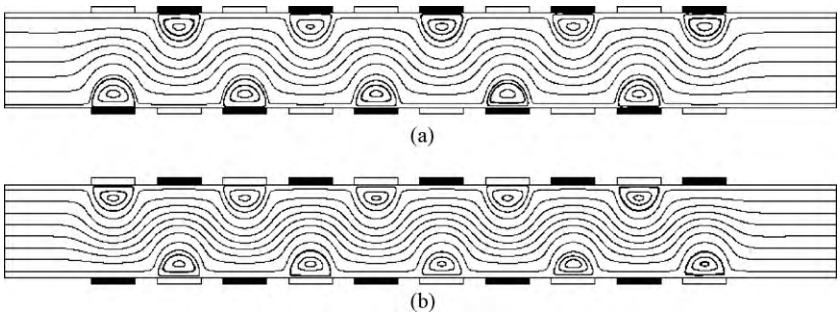

Fig. 3. Flow streamlines. (a) Zeta potential on wall surfaces of filled blocks is given as $\zeta = +|\zeta_h|$ while zeta potential on wall surfaces of unfilled blocks is set as $\zeta = -|\zeta_h|$. (b) Zeta potential on wall surfaces of filled blocks is given as $\zeta = -|\zeta_h|$ while zeta potential on wall surfaces of unfilled blocks is set as $\zeta = +|\zeta_h|$. Note that ζ_h has a value of $\zeta_h = 75$ mV. Note also that the zeta potential on the remaining wall surfaces of the channel is specified as $\zeta = -75$ mV. In addition, the length of the heterogeneous surface patterns is given as $L_{het} = 1.0W$.

complex flow behavior [24]. Generally speaking, the time-varying zeta potentials can be induced using the field effect [28]. Many previous experimental and numerical studies have shown that an effective mixing performance can be obtained through the specification of an appropriate time-switching period to modulate the variation of the zeta potential [29–31].

The majority of the active mixing schemes presented in the literature mix the species using some form of periodic perturbation source. However, aperiodic oscillating sources have a number of advantages, including the generation of a random-like oscillating effect, an oscillatory characteristic comprising multiple oscillating frequencies, and so on. Accordingly, the present study proposes an enhanced micromixing scheme in which the species are perturbed by an aperiodic oscillating source derived from the Sprott system [32]. In the proposed approach, the local zeta potential on the microchannel wall varies over time in accordance with the oscillatory behavior of the Sprott system. The resulting time-varying zeta potentials prompt the formation of irregularly alternating flow recirculations in the microchannel which perturb the species streams and improve the mixing efficiency as a result. A series of simulations are performed to examine the respective effects of the magnitude of the time-varying zeta potential, the length of the heterogeneous surface zeta potential patterns, and the alternating frequency of the zeta potential on the fluid flow characteristics and corresponding mixing performance.

2. Mathematical formulation

Fig. 1 presents a schematic illustration of the micromixer considered in the present analysis. As shown, the microchannel has a total length L, a width W, a mixing region of length L_{mix}, and an injection channel of length L_i. Furthermore, the mixing region of the channel incorporates ten pairs of heterogeneous surface zeta potential patches of length L_{het}, where each patch is separated from its neighbors by homogenous surface zeta potential patches of length L_{hom}.

Table 1
Physical properties of solution.

Symbol	Description	Value
e	Charge of an electron	$1.6021 \times 10^{-19} C$
D	Diffusion coefficient	$1 \times 10^{-11}\ m^2\ s^{-1}$
K_b	Boltzmann constant	$1.38 \times 10^{-23}\ J\ K^{-1}$
T	Absolute temperature	298.16 K
z	Valence	1
ε	Dielectric constant	80
ε_0	Permittivity of vacuum	$8.854 \times 10^{-12}\ F\ m^{-1}$
μ	Viscosity of fluid	$10^{-3}\ N\ s\ m^{-2}$
ρ	Density of fluid	$10^{3}\ kg\ m^{-3}$

2.1. Governing equations

In analyzing the sample flow within the microchannel shown in Fig. 1, the governing equations are simplified via the following assumptions: (i) the sample solutions are incompressible, Newtonian liquids; (ii) the gravitational and buoyancy effects are sufficiently small to be ignored; (iii) the two samples have the same constant diffusion coefficient; (iv) no chemical reactions take place; and (v) the channel height is neglected such that the flow fields are two-dimensional [33]. The various governing equations are described in the sections below.

2.1.1. Poisson–Boltzmann equation

According to electrostatics theory, the electrical double layer (EDL) potential distribution can be described by the Poisson–Boltzmann equation, which in the case of symmetric electrolytes such as KCl has the form

$$\nabla^2\psi = \frac{2n_0 ze}{\varepsilon\varepsilon_0}\sinh\left(\frac{ze}{k_bT}\psi\right) \tag{1}$$

where ψ is the potential induced by the charge on the walls, n_0 is the bulk concentration of the ions, z is the ionic valence, e is the elementary charge, ε is the dielectric constant of the electrolyte solution, ε_0 is the permittivity of a vacuum, k_b is the Boltzmann constant, and T is the absolute temperature.

2.1.2. Laplace equation

The distribution of the externally applied electric potential in the microchannel is described by the following Laplace equation:

$$\nabla^2\phi = 0, \tag{2}$$

where ϕ is the applied electrical potential. Note that the electric field is equivalent to $E = -\nabla\phi$.

2.1.3. Navier–Stokes equations with electrokinetic driving body force term

In a microchannel filled with an aqueous solution, the application of an external electric field induces an electrokinetic body force near the wall surface which affects the characteristics of the fluid flow. Therefore, the Navier–Stokes equations must be modified to take account of the electrokinetic body force. The modified Navier–Stokes equations have the form

$$\nabla\cdot\vec{V} = 0, \tag{3}$$

$$\rho\left[\frac{\partial\vec{V}}{\partial t} + (\vec{V}\cdot\nabla)\vec{V}\right] = -\nabla P + \mu\nabla^2\vec{V} + \vec{F}_E, \tag{4}$$

where ρ is the fluid density, $\vec{V}$ is the velocity vector with components u and v in the x- and y-directions, respectively, P is the

pressure, μ is the fluid viscosity, and $\vec{F}_E$ is the electrokinetic driving body force and is defined as $\vec{F}_E = 2n_0 ze \sinh((ze/k_bT)\psi)\nabla(\psi+\phi)$ [10,21].

2.1.4. Concentration distribution equation

Assuming that the electrophoretic effect is neglected, the species transport can be described by the following convection-diffusion equation:

$$\frac{\partial C}{\partial t} + (\vec{V}\cdot\nabla)C = D\nabla^2 C, \tag{5}$$

where C is the species concentration and D is the diffusion coefficient.

2.2. Initial and boundary conditions

In simulating the species flow in the microchannel shown in Fig. 1, it is assumed that species A and B are initially static and completely fill the upper and lower regions of the microchannel, respectively. In setting the boundary conditions, a constant electric field is applied along the microchannel, and a time-varying zeta potential is applied to the heterogeneous surface zeta patterns. Furthermore, a slip velocity condition is applied at the wall surfaces. The initial and boundary conditions are formulated as follows:

Initial conditions

$$\vec{V} = 0, \quad C = C_A \text{ or } C_B. \tag{6a}$$

Boundary conditions

Inlet

$$\phi = \phi_{in}, \quad P = 0, \quad C = C_{in}. \tag{6b}$$

Outlet

$$\phi = \phi_{out}, \quad P = 0, \quad \nabla C\cdot\vec{n} = 0. \tag{6c}$$

Wall surfaces

$$\nabla\phi\cdot\vec{n} = 0, \quad \vec{V} = \vec{V}_{HS}, \quad \nabla C\cdot\vec{n} = 0. \tag{6d}$$

Note that in the equations above, ϕ_{in} and ϕ_{out} are the applied electric potentials at the inlet and outlet, respectively; $\vec{V}_{HS}$ is the Helmholtz–Smoluchowski slip velocity and is equal to $\vec{V}_{HS} = -(\varepsilon\varepsilon_0\zeta/\mu)E$ [34]; ζ is the zeta potential on the wall surface; E is the magnitude of the electric field; C_{in} is the species concentration in the inlet; and n denotes the normal direction to the wall surface. Note that the zeta potential is specified as $\zeta = -|\zeta_w|$ and $\zeta = \pm|\zeta_h(t)|$ for the homogeneous and heterogeneous surface patterns, respectively.

2.3. Oscillatory sources and mixing scheme protocol

In the mixing scheme proposed in this study, the time-varying zeta potential applied to the heterogeneous surface patterns is modulated by an aperiodic oscillating source generated using the Sprott system [32]. In other words, the oscillating source has the form

$$\dot{x}_1 = kx_2, \tag{7a}$$

$$\dot{x}_2 = kx_3, \tag{7b}$$

$$\dot{x}_3 = k[-p_1x_1 - p_2x_2 - p_3x_3 + p_4\,\mathrm{Sign}(x_1)], \tag{7c}$$

where x_1, x_2 and x_3 are the oscillatory sources, $p_1 = 1.2$, $p_2 = 1.0$, $p_3 = 0.6$ and $p_4 = 2.0$ are the system parameters, and k is the scaling factor. In the present study, the Sprott system is solved using the fourth-order Runge–Kutta algorithm. Fig. 2(a)–(c) presents the oscillatory orbits of x_1 for initial values of $(x_1, x_2, x_3) = (0.1, 0.1, 0.1)$ and scaling factors of $k = 10$, 50 and 100, respectively. It can be seen that the oscillatory frequency of x_1 can be easily adjusted via the application of a suitable scaling factor. Note that the oscillatory behavior of the Sprott system can be generated using simple electric circuits [32].

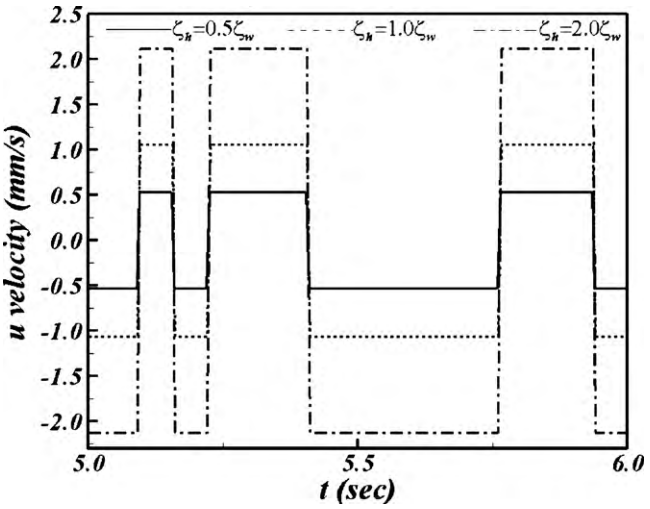

Fig. 4. Evolution of u-velocity component near wall surface in center of heterogeneous surface zeta potential patches for three different values of zeta potential. Note that the scaling factor is given as $k = 50$.

In accordance with the Sprott system, the variations over time of the zeta potentials acting on the surfaces of the filled and unfilled blocks in Fig. 1 are specified as follows:

Filled blocks

$$\zeta = \begin{cases} -|\zeta_h| & \text{if} \quad x_1 > 0 \\ +|\zeta_h| & \text{if} \quad x_1 \le 0 \end{cases}, \tag{8a}$$

Unfilled blocks

$$\zeta = \begin{cases} +|\zeta_h| & \text{if} \quad x_1 > 0 \\ -|\zeta_h| & \text{if} \quad x_1 \le 0 \end{cases}, \tag{8b}$$

where ζ_h is the specified value of the zeta potential.

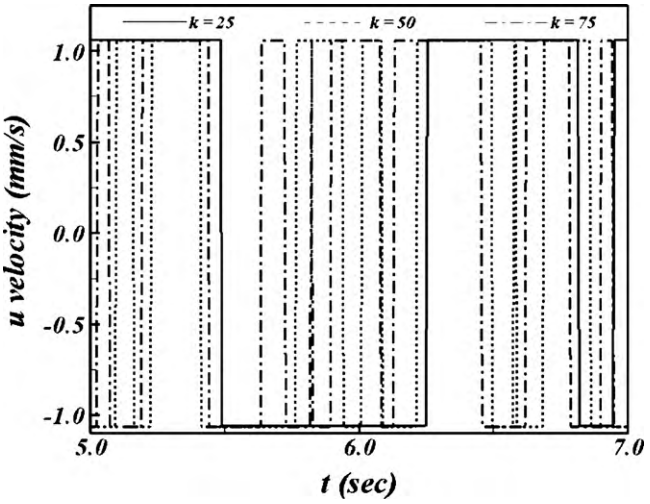

Fig. 5. Evolution of u-velocity component near wall surface in center of heterogeneous surface zeta potential patches for three different values of scaling factor. Note that the zeta potential on the heterogeneous surfaces is given as $\zeta_h = 75$ mV.

2.4. Numerical method

In simulating the sample flows within the microchannel shown in Fig. 1, the governing equations (Eqs. (2)–(5)) and initial and boundary conditions were solved numerically using the finite-volume method [35]. Note that an assumption was made that the EDL thickness was significantly less than the characteristic length of the microchannel. Thus, in performing the simulations, the variation of the velocity within the EDL was neglected and the Helmholtz–Smoluchowski slip velocity was applied at the wall surfaces [34]. As a result, the electrokinetic body force term in Eq. (4) was neglected, causing the Poisson–Boltzmann equation (Eq. (1)) to become redundant. Consequently, the complexity of the solution procedure was significantly reduced. The transient time terms and convection terms in Eqs. (4) and (5) were discretized using the fully-implicit method and a second-order scheme, respectively. The velocity and pressure fields were coupled using the SIMPLE C algorithm [36]. The discretized algebraic equations were solved using the TDMA (tri-diagonal matrix algorithm) scheme. In the solution procedure, the Laplace equation (Eq. (2)) was solved to obtain the distribution of the externally applied electric potential within the microchannel, and the variation of the Helmholtz–Smoluchowski slip velocity at the wall surfaces over time was then calculated in accordance with the specified zeta potential and the externally applied electric field. Thereafter, the Navier–Stokes equations (Eqs. (3) and (4)) and convection-diffusion equation (Eq. (5)) were solved to obtain the evolution over time of the flow field and species concentration field. Finally, at each time step, the mixing efficiency was estimated following the convergence of the species concentration field. Note that prior to the simulations, a sensitivity analysis was performed to establish a suitable mesh size and time step.

2.5. Mixing efficiency

The performance of the proposed mixing scheme was quantified by evaluating the mixing efficiency (η_m) at a specified cross-section of the microchannel in accordance with [25]

$$\eta_m = \left[1 - \frac{\int_{-W/2}^{W/2} |C - C_\infty| \, dy}{\int_{-W/2}^{W/2} |C_0 - C_\infty| \, dy}\right] \times 100\%, \quad (9)$$

where C is the species concentration; C_∞ is the species concentration in the perfectly mixed condition, and C_0 is the species concentration in the completely unmixed condition. Thus, a mixing efficiency of $\eta_m = 100\,\%$ indicates a perfectly mixed state, while a mixing efficiency of $\eta_m = 0\,\%$ indicates a completely unmixed state.

3. Results and discussion

The model presented in Fig. 1 was used as the basis for a series of numerical simulations designed to examine the effects of the aperiodic spatio-temporal variations of the zeta potential on the fluid flow characteristics and corresponding mixing performance. In the simulations, the width of the channel was specified as $W = 50\,\mu m$, the length of the injection channel was set as $L_i = 10W$, and the

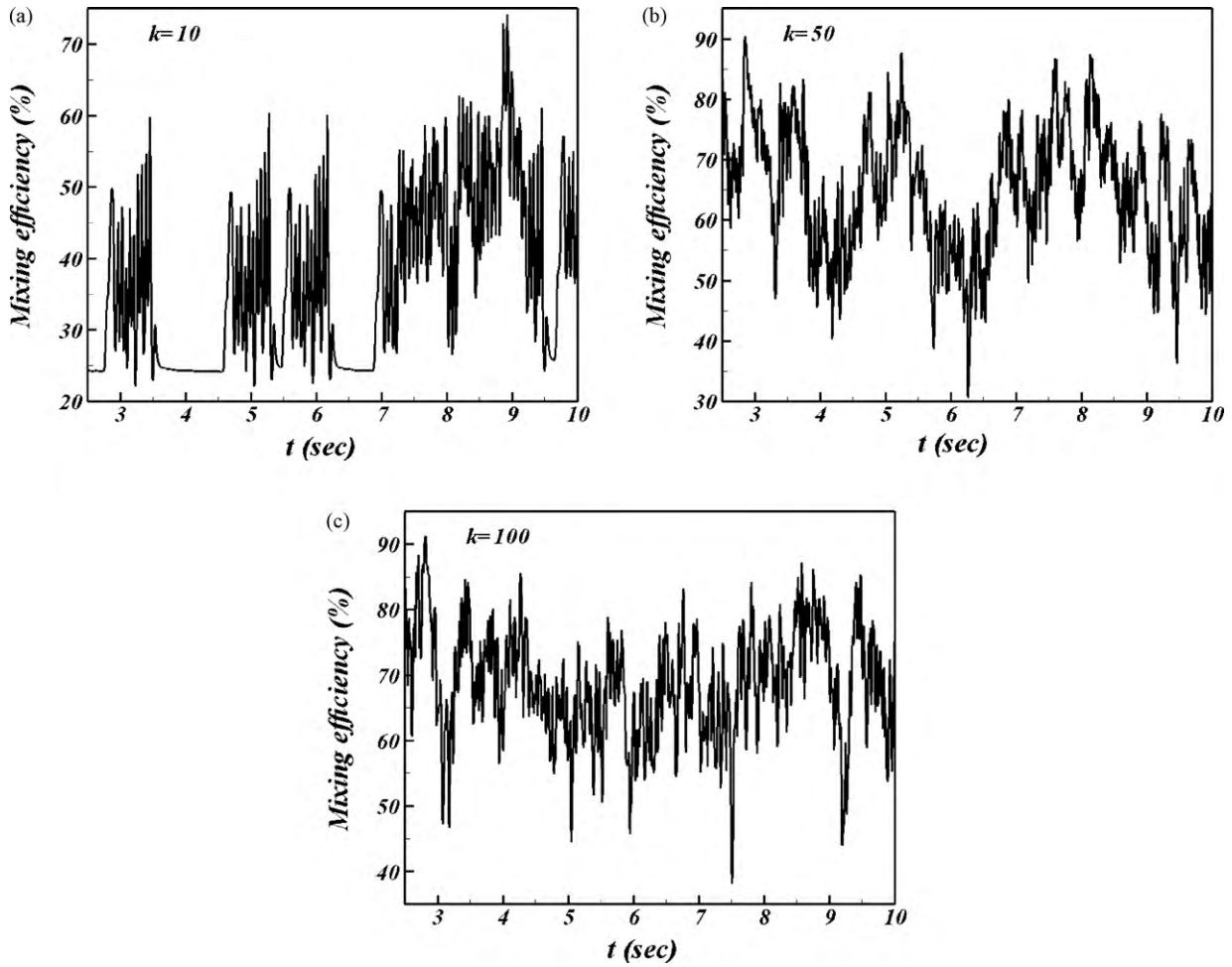

Fig. 6. Evolution of mixing efficiency at $x = 2000\,\mu m$ as function of time for scaling factors of: (a) $k = 10$, (b) $k = 50$, and (c) $k = 100$. Note that the zeta potential on the heterogeneous surfaces is given as $\zeta_h = 75$ mV. Note also that the length of the heterogeneous surface patterns is set as $L_{het} = 1.0W$.

length of the homogeneous surface zeta patches in the mixing section was given as $L_{hom} = 0.5W$. In addition, it was assumed that the microchannel was made of silica glass and had a zeta potential of $\zeta = -75$ mV. The intensity of the externally applied electric field was set as $E = 200$ V/cm. Furthermore, the working fluids were assumed to be aqueous solutions. The physical properties of the solutions are summarized in Table 1. Finally, the Reynolds number ($Re = \rho \bar{V}_{HS} W/\mu$) and Peclet number ($Pe = \bar{V}_{HS} W/D$) of the sample flows were specified as $Re = 5 \times 10^{-2}$ and $Pe = 5.3 \times 10^{3}$, respectively.

Fig. 3 presents the flow streamline distributions within the microchannel for two different assignments of the zeta potential on the heterogeneous wall surfaces. Note that the zeta potential on the homogeneous wall surfaces is assumed to be negative. It can be seen that in both cases, a series of flow recirculations are generated along the length of the mixing channel. In electroosmotic flow, an electrokinetic driving force is induced by the interaction between the EDL potential and the externally applied electric field. This driving force acts only on the fluid near the walls of the microchannel. However, the bulk fluid is also dragged into motion via a momentum coupling effect with the driven fluid. If the external electric field has a constant distribution along the microchannel and a uniform zeta potential is applied along the channel wall, the electrokinetic driving force near the wall acts in the same direction at all points along the microchannel. Consequently, all of the bulk fluid moves in the same direction and flow recirculations are not induced. Under such circumstances, a poor species mixing is obtained since the species streams are mixed as the result of diffusion alone. However, in the case shown in Fig. 3, the external electric field is constant along the length of the microchannel and a non-uniform zeta potential is applied along the wall surfaces. The fluid near the positive zeta potential surfaces moves in the opposite direction to that near the negative zeta potential surfaces, and thus local flow recirculations are formed near the positive zeta potential surfaces in order to satisfy the continuity condition. These flow recirculations perturb the two species streams and enhance the mixing between them as a result. When time-varying zeta potentials are applied to the local wall surface in accordance with the Sprott system described in Section 2.3, the two flow recirculation patterns shown in Fig. 3 switch alternately at irregular intervals. The switching of the two recirculation structures results in a repeated aperiodic folding and stretching of the species streams, and therefore leads to a significant improvement in the mixing efficiency.

Fig. 4 shows the effect of the magnitude of the zeta potential on the time-varying flow velocity near the wall surface in the center of the heterogeneous zeta patches. In electroosmotic flow, the direction and magnitude of the flow velocity induced by the electrokinetic driving force are determined by the Helmholtz–Smoluchowski equation. Hence, given the assumption of a constant external electric field, the electroosmotic velocity in the region of the heterogeneous surface patches acts in the same direction (when the surface zeta potential is negative) or the opposite direction (when the surface zeta potential is positive) as that in the region of the homogeneous surface patches. When the variation of the electroosmotic velocity on the heterogeneous surface patches is as shown in Fig. 4, an irregularly alternating series of recirculating flow structures are generated over time within the mixing region, prompting a stirring of the species. According to the Helmholtz–Smoluchowski equation, given a constant external electric field, the electroosmotic velocity is proportional to the magnitude of the surface zeta potential. Therefore, when a stronger time-varying zeta potential is applied to the heterogeneous surface zeta patches, a larger acceleration force (when the surface zeta potential is negative) or deceleration force (when the surface zeta potential is positive) is produced. Consequently, the size of the recirculation structures near the heterogeneous surface zeta patches is increased and a further improvement in the mixing performance is obtained. By contrast, a smaller zeta potential results in smaller recirculation structures, and therefore reduces the mixing efficiency.

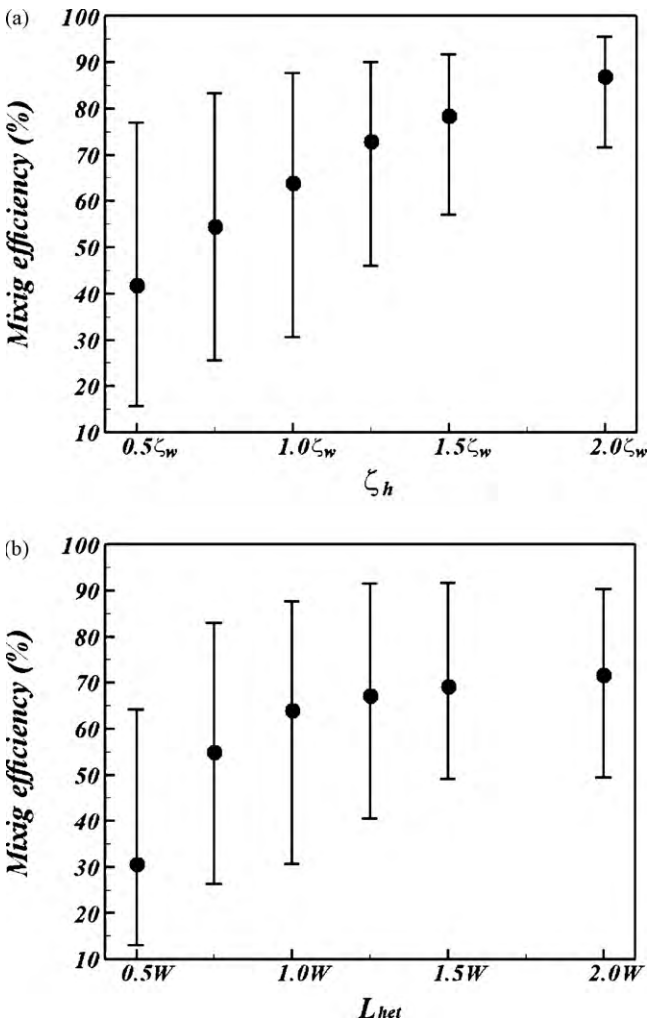

Fig. 7. Average mixing efficiency at $x = 2000$ μm over time $t = 5$–10 s when (a) length of heterogeneous patterns is set as $L_{het} = 1.0W$, and (b) magnitude of heterogeneous surface zeta potential is given as $\zeta_h = 1.0\zeta_w$. Note that the scaling factor is set as $k = 50$ in both cases. Note also that • indicates the average value of the mixing efficiency, while the error bars indicate the variation range of the mixing efficiency.

Fig. 5 illustrates the evolution over time of the u-velocity component near the wall surface in the center of the heterogeneous surface zeta potential patches for different values of the scaling factor. It can be seen that the alternating frequency at which the electroosmotic velocity varies increases as the value of the scaling factor is increased due to the corresponding increase in the aperiodic oscillatory frequency of the oscillatory source. In other words, the results presented in Fig. 5 imply that an improved species perturbation effect can be achieved by increasing the oscillating frequency of the oscillatory source to an appropriate value.

Fig. 6(a)–(c) illustrate the evolution over time of the mixing efficiency at $x = 2000$ μm (cross-section $A - A'$ in Fig. 1) for scaling factors of $k = 10$, 50 and 100, respectively. Since the formation of the recirculating structures within the mixing region takes place aperiodically, an irregular perturbation of the species occurs. Therefore, it can be seen that the mixing efficiency within the microchannel varies irregularly over time at all values of the scaling factor. However, at lower values of the scaling factor, the switching frequency of the recirculation structures reduces. Consequently, the species

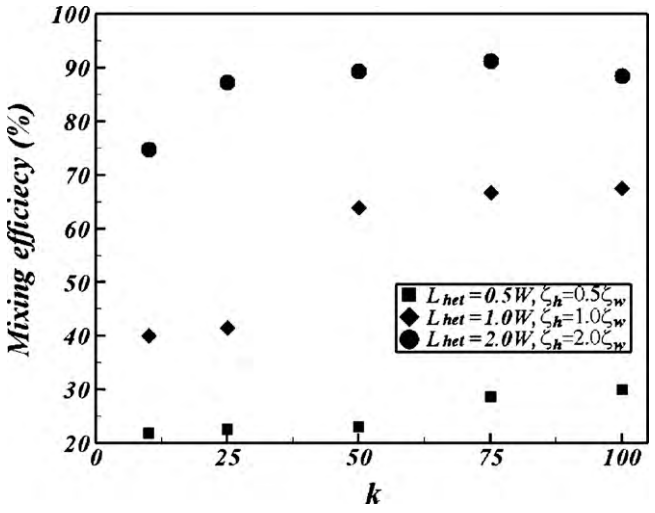

Fig. 8. Average mixing efficiency at $x = 2000\,\mu m$ over time $t = 5–10\,s$ for different scaling factors, heterogeneous surface zeta potential pattern lengths, and zeta potential magnitudes.

are stirred less vigorously as they pass through the mixing region. As a result, a relatively poor mixing performance is obtained (see Fig. 6(a)). However, as the scaling factor is increased, the frequency at which the recirculation structures alternate also increases. Thus, a more vigorous stirring of the species takes place and a more effective mixing performance is obtained as a result (see Fig. 6(b) and (c)). Overall, the results presented in Fig. 6 confirm that the mixing performance can be improved by applying an appropriate scaling factor to the aperiodic oscillating sources used to modulate the variation of the zeta potential on the heterogeneous surfaces.

Fig. 7(a) and (b) shows the average mixing efficiency at $x = 2000\,\mu m$ over the time interval $t = 5–10\,s$ as a function of the magnitude of the heterogeneous zeta potential and the length of the heterogeneous surface zeta potential patterns, respectively. It is seen that the mixing efficiency increases with both an increasing zeta potential and an increasing heterogeneous zeta pattern length. As discussed earlier in relation to Fig. 4, the size of the recirculation structures reduces as the zeta potential is reduced, causing a corresponding reduction in the mixing performance. However, as the magnitude of the zeta potential is increased, the size of the flow recirculations also increases, and thus the mixing efficiency is correspondingly improved. Furthermore, as the length of the heterogeneous surface zeta potential patterns is increased, the extent of the recirculations also increases, and hence a further improvement in the mixing performance is obtained.

Fig. 8 shows the average mixing efficiency at $x = 2000\,\mu m$ over the time interval $t = 5–10\,s$ for different values of the scaling factor, zeta potential magnitude, and heterogeneous zeta pattern length. The results confirm that the mixing efficiency not only increases with an increasing zeta potential and heterogeneous zeta potential pattern length, but also with an increasing scaling factor. As discussed earlier, the recirculating structures within the mixing region are formed irregularly over time due to the aperiodic variations of the oscillating source. As a result, the two species streams are also stirred irregularly. For a given heterogeneous surface zeta potential and heterogeneous zeta pattern length, the mixing efficiency attains its maximum value once the scaling factor exceeds a certain threshold value. From inspection, it can be seen that the mixing efficiency exceeds 90% when the magnitude of the heterogeneous surface zeta potential is twice that of the homogeneous surface zeta potential, the length of the heterogeneous surface zeta potential patterns is equal to twice the channel width, and the scaling factor exceeds 25.

4. Conclusions

This study has proposed a novel micromixing scheme in which the species are mixed by the flow recirculation structures induced by aperiodic spatial–temporal variations of the zeta potential applied to the microchannel walls. In the proposed mixing method, the variation of the zeta potential over time is modulated by an aperiodic oscillating source defined in accordance with the Sprott system. The effects on the mixing performance of the heterogeneous zeta pattern length, the magnitude of the time-varying zeta potential, and the switching frequency of the zeta potential have been systematically examined using a numerical simulation approach. The simulation results have shown that the temporal- and spatial-varying zeta potential distribution within the microchannel results in the formation of a series of irregularly alternating recirculation structures which prompt the repeated stretching and folding of the species streams and therefore enhance the mixing performance. Moreover, it has been shown that the mixing efficiency can be improved by increasing the magnitude of the heterogeneous surface zeta potential and the length of the heterogeneous zeta potential surface patterns. In addition, the mixing performance can be further improved by increasing the aperiodic alternating frequency of the zeta potential to an appropriate value. Overall, the simulation results show that the proposed mixing scheme can achieve a mixing efficiency of more than 90% given an appropriate specification of the magnitude of the heterogeneous surface zeta potential, the length of the heterogeneous surface zeta patterns, and the aperiodic oscillating frequency of the oscillating source used to modulate the zeta potential.

Acknowledgment

The authors gratefully acknowledge the financial support provided to this study by the National Science Council of Taiwan under Grant No. NSC-98-2221-E-006-176-MY2.

References

[1] A.D. Stroock, S.K.W. Dertinger, A. Ajdari, I. Mezic, H.A. Stone, G.M. Whitesides, Chaotic mixer for microchannels, Science 295 (2002) 647–651.
[2] Y.J. Johnson, D. Ross, L.E. Locascio, Rapid microfluidic mixing, Anal. Chem. 74 (2002) 45–51.
[3] S.P. Kee, A. Gavriilidis, Design and characterisation of the staggered herringbone mixer, Chem. Eng. J. 142 (2008) 109–121.
[4] R.H. Liu, M.A. Stremler, K.V. Sharp, M.G. Olsen, J.G. Santiago, R.J. Adrian, H. Aref, D.J. Beeber, Passive mixing in a three-dimensional serpentine microchannel, J. Microelectromech. Syst. 9 (2000) 190–197.
[5] J.M. Park, D.S. Kim, T.G. Kang, T.H. Kwon, Improved serpentine laminating micromixer with enhanced local advection, Microfluid. Nanofluid. 4 (2008) 513–523.
[6] M.A. Ansari, K.Y. Kim, Parametric study on mixing of two fluids in a three-dimensional serpentine microchannel, Chem. Eng. J. 146 (2009) 439–448.
[7] F. Schonfeld, V. Hessel, C. Hofmann, An optimised split-and-recombine micromixer with uniform 'chaotic' mixing, Lab Chip 4 (2004) 65–69.
[8] S. Hardt, F. Pennemann, F. Schonfeld, Theoretical and experimental characterization of a low-Reynolds number split-and-recombine mixer, Microfluid. Nanofluid. 2 (2006) 237–248.
[9] V. Mengeaud, J. Josserand, H.H. Girault, Mixing processes in a zigzag microchannel: finite element simulations and optical study, Anal. Chem. 74 (2002) 4279–4286.
[10] C.K. Chen, C.C. Cho, Electrokinetically-driven flow mixing in microchannels with wavy surface, J. Colloid Interface Sci. 312 (2007) 470–480.
[11] C.K. Chen, C.C. Cho, A combined active/passive scheme for enhancing the mixing performance of microfluidic devices, Chem. Eng. Sci. 63 (2008) 3081–3087.
[12] X. Niu, Y.K. Lee, Efficient spatial-temporal chaotic mixing in microchannels, J. Micromech. Microeng. 13 (2003) 454–462.
[13] A. Dodge, M.C. Jullien, Y.K. Lee, X. Niu, F. Okkels, P. Tabeling, An example of a chaotic micromixer: the cross-channel micromixer, C. R. Phys. 5 (2004) 557–563.
[14] Y.K. Lee, C. Shih, P. Tabeling, C.M. Ho, Experimental study and nonlinear dynamic analysis of time-periodic micro chaotic mixers, J. Fluid Mech. 575 (2007) 425–448.

[15] Z. Tang, S. Hong, D. Djukic, V. Modi, A.C. West, J. Yardley, R.M. Osgood, Electrokinetic flow control for composition modulation in a microchannel, J. Micromech. Microeng. 12 (2002) 870–877.
[16] T.J. Coleman, D. Sinton, A sequential injection microfluidic mixing strategy, Microfluid. Nanofluid. 1 (2005) 319–327.
[17] M.H. Oddy, J.G. Santiago, J.C. Mikkelsen, Electrokinetic instability micromixing, Anal. Chem. 73 (2001) 5822–5832.
[18] S.M. Shin, I.S. Kang, Y.K. Cho, Mixing enhancement by using electrokinetic instability under time-periodic electric field, J. Micromech. Microeng. 15 (2006) 455–462.
[19] F.R. Phelan, P. Kutty, J.A. Pathak, An electrokinetic mixer driven by oscillatory cross flow, Microfluid. Nanofluid. 5 (2008) 101–118.
[20] J.R. Pacheco, K.P. Chen, A. Pacheco-Vega, B. Chen, M.A. Hayes, Chaotic mixing enhancement in electro-osmotic flows by random period modulation, Phys. Lett. A 372 (2008) 1001–1008.
[21] C.K. Chen, C.C. Cho, Electrokinetically driven flow mixing utilizing chaotic electric fields, Microfluid. Nanofluid. 5 (2008) 785–793.
[22] C.L. Chen, H.T. Yau, C.C. Cho, C.K. Chen, Enhancement of microfluidic mixing using harmonic and chaotic electric fields, Int. J. Nonlinear Sci. Numer. Simul. 10 (2009) 1545–1553.
[23] A. Ajdari, Electro-osmosis on inhomogeneous charged surfaces, Phys. Rev. Lett. 75 (1995) 755–758.
[24] S. Qian, H.H. Bau, A chaotic electroosmotic stirrer, Anal. Chem. 74 (2002) 3616–3625.
[25] D. Erickson, D. Li, Influence of surface heterogeneity on electrokinetically driven microfluidic mixing, Langmuir 18 (2002) 1883–1892.
[26] A.D. Stroock, G.M. Whitesides, Controlling flows in microchannels with patterned surface charge and topography, Accounts Chem. Res. 36 (2003) 597–604.
[27] E. Biddiss, D. Erickson, D. Li, Heterogeneous surface charge enhanced micromixing for electrokinetic flows, Anal. Chem. 76 (2004) 3208–3213.
[28] R.B.M. Schasfoort, S. Schlautmann, J. Hendrikse, A. Van den Berg, Field-effect flow control for microfabricated fluidic networks, Science 286 (1999) 942–945.
[29] C.Y. Lee, G.B. Lee, L.M. Fu, K.H. Lee, R.J. Yang, Electrokinetically driven active micro-mixers utilizing zeta potential variation induced by field effect, J. Micromech. Microeng. 14 (2004) 1390–1398.
[30] C.C. Chang, R.J. Yang, Chaotic mixing in electro-osmotic flows driven by spatiotemporal surface charge modulation, Phys. Fluids 21 (2009) 052004.
[31] H.J. Kim, A. Beskok, Numerical modeling of chaotic mixing in electroosmotically stirred continuous flow mixers, J. Heat Transfer 131 (2009) 092403.
[32] H.C. Chen, J.F. Chang, J.J. Yau, T.L. Liao, EP-based PID control design for chaotic synchronization with application in secure communication, Exp. Syst. Appl. 34 (2008) 1169–1177.
[33] N.A. Patankar, H.H. Hu, Numerical simulation of electroosmotic flow, Anal. Chem. 70 (1998) 1870–1881.
[34] R.F. Probstein, Physicochemical Hydrodynamics an Introduction, John Wiley & Sons, New York, 1994.
[35] S.V. Patankar, Numerical Heat Transfer and Fluid Flow, McGraw-Hill, New York, 1980.
[36] J.P. Van Doormal, G.D. Raithby, Enhancement of the SIMPLE method for predicting incompressible fluid flows, Numer. Heat Transfer 7 (1984) 147–163.